

W-CDMA Uplink Capacity and Interference Statistics of a Long Groove-Shaped Road Microcells Using A Hybrid Propagation Model

Bazil TAHA-AHMED, Miguel CALVO-RAMÓN, Leandro de HARO-ARIET

Departamento Sistemas, Señales y Radiocomunicaciones, ETSI Telecomunicación,
Universidad Politécnica de Madrid, Ciudad Universitaria, Madrid, 28040, Spain

bazil@gr.ssr.upm.es

Abstract. The uplink capacity and the interference statistics of the sectors of a long groove-shaped road W-CDMA microcell are studied. A model of 9 microcells in a groove-shaped road is used to analyze the uplink. A hybrid model for the propagation is used in the analysis. The capacity and the interference statistics of the cell are studied for different sector ranges, different specific attenuation factors, different antenna side lobe levels and different bend losses.

Keywords

W-CDMA, cells capacity, shadowing.

1. Introduction

CDMA is characterized as being interference-limited, so reducing the interference results in increasing the capacity. Three factors are mainly used to reduce the interference: power control (PC), voice activity monitoring and sectorization. It is well known that urban microcell shapes may approximately follow the street pattern and that it is possible to have cigar-shaped cells [1]. This type of cells appears also in tunnels and groove-shaped roads.

The conditions that describe the long groove road cigar-shaped microcells under this study are

- The number of directive sectors of the cigar-shaped cell is two and a directive antenna is used in each sector.
- The sector has typically a range of about one kilometer.
- The groove length is of the order 3 to 5 km.
- The user speed in the tunnel can reach 120 km/h.

Fig. 1 shows the coverage of the sector and the cigar-shaped cell.

Min *et al* studied the performance of the CDMA highway microcells [2]. Hashem *et al* studied the capacity and

the interference statistics for hexagonal cells using a propagation exponent of 4.0 [3]. Ahmed *et al* studied the capacity and interference statistics of highway cigar-shaped microcells [4]. In [5], Ahmed *et al* studied the capacity and interference statistics of a tunnel cigar-shaped microcells using a two exponent propagation model. In this work, we introduce a model for cigar-shaped cells in groove road, with general propagation exponent using a two-slope attenuation model and then investigate the sector capacity and interference statistics of the uplink.

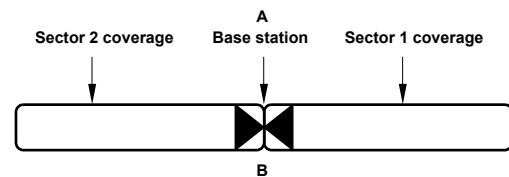


Fig. 1. The sector and cell coverage. A – the sector coverage. B – the cell coverage.

The paper has been organized as follows. In section 2, the propagation model is given. Section 3 explains the method to obtain the capacity and the interference statistics of the uplink. Numerical results are presented in section 4. Finally, conclusions are drawn in section 5.

2. The Propagation Model

From the measurements presented in [6], the propagation model in the groove road can be approximated by a two or more slopes model applicable in the microwave frequency range. A hybrid propagation model with lognormal shadowing is used in our calculations. The propagation exponent until the break point R_b is assumed to be s . For a distance r greater than R_b , the signal is assumed to be attenuated by a specific attenuation factor of n dB/m. In this way, the path loss is given by:

$$L_p(dB) = K + 10 \log r^s + L_1 + \xi_1, \quad (1)$$

$$L_p(dB) = K + 10 \log R_b^s + n(r - R_b) + L_2 + \xi_2. \quad (2)$$

Eqn. (1) is valid for $r \leq R_b$, and eqn. (2) is used for $r > R_b$.

In (1) and (2), s is the propagation exponent until R_b , K is the attenuation at a distance of 1 m, n is the specific attenuation after R_b , L_i is the tunnel bend loss between the source and the observation point d if applicable, ξ_1 and ξ_2 are Gaussian random variables of zero-mean and a standard deviation of σ_1 and σ_2 respectively.

For the tunnel environment, r is the distance between the base station of the cell C and the mobile and the breakpoint distance R_b is given by:

$$R_b \approx a^2 / \lambda \quad (3)$$

where a is the groove road width, normally 6 to 8 meters, and λ is the wavelength. Typical value of s is around 2 and $n = 0.02 - 0.06$ dB/m [6] and [7].

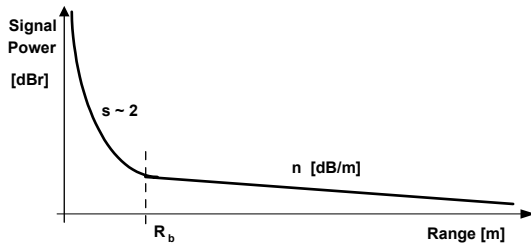


Fig. 2. The field intensity profile.

Fig. 2 depicts the general shape of the propagation loss profile for the groove road microcell.

3. Uplink Analysis

The configuration of the multi-microcells model is shown in Fig. 3. In this case, each cell controls the transmitted power of its users. The sector range is assumed to be R . If the interfering user i is at a distance r_{im} from its base station and at a distance r_{id} from the base station of the reference cell d as shown in Fig. 4, then the normalized interference signal $L(r_{id}, r_{im})$ due only to the distance and bends is given as:

$$L(r_{id}, r_{im}) = \frac{10^{\lfloor 10 \log r_{im}^s + L_{bim} \rfloor / 10}}{10^{\lfloor 10 \log r_{id}^s + L_{bid} \rfloor / 10}} \quad (4)$$

for $r_{id} \leq R_b$ and $r_{im} \leq R_b$;

$$L(r_{id}, r_{im}) = \frac{10^{\lfloor 10 \log r_{im}^s + L_{bim} \rfloor / 10}}{10^{\lfloor 10 \log R_b^s + n(r_{id} - R_b) + L_{bid} \rfloor / 10}} \quad (5)$$

for $r_{id} > R_b$ and $r_{im} \leq R_b$;

$$L(r_{id}, r_{im}) = \frac{10^{\lfloor 10 \log R_b^s + n(r_{im} - R_b) + L_{bim} \rfloor / 10}}{10^{\lfloor 10 \log r_{id}^s + L_{bid} \rfloor / 10}} \quad (6)$$

for $r_{id} \leq R_b$ and $r_{im} > R_b$;

$$L(r_{id}, r_{im}) = \frac{10^{\lfloor n(r_{im} - R_b) + L_{bim} \rfloor / 10}}{10^{\lfloor n(r_{id} - R_b) + L_{bid} \rfloor / 10}} \quad (7)$$

for $r_{id} > R_b$ and $r_{im} > R_b$.

In the above-given equations, L_{bij} is the bend loss between the user i and the base station j .

Now the normalized interference signal $I(r_{id}, r_{im})$ due to the distance, the bends and shadowing is given by

$$I(r_{id}, r_{im}) = 10^{(\xi_{id} - \xi_{im}) / 10} L(r_{id}, r_{im}) \quad (8)$$

where ξ_{id} and ξ_{im} are given as

- $\xi_{id} = \xi_1$ and $\xi_{im} = \xi_1$ for $r_{id} \leq R_b$ and $r_{im} \leq R_b$;
- $\xi_{id} = \xi_2$ and $\xi_{im} = \xi_1$ for $r_{id} > R_b$ and $r_{im} \leq R_b$;
- $\xi_{id} = \xi_1$ and $\xi_{im} = \xi_2$ for $r_{id} \leq R_b$ and $r_{im} > R_b$;
- $\xi_{id} = \xi_2$ and $\xi_{im} = \xi_2$ for $r_{id} > R_b$ and $r_{im} > R_b$.

We will divide the total intercellular interference ($I_{inter,t}$) in the interference from users in the S0 region (I_{S0}) and the interference from users in the S1 region (I_{S1}), where the regions are shown in Fig. 3. We will find the interference at the right sector (drawn in black) of the central cell C1 assuming it to be the reference cell d . We assume that users in the region S0, communicate with the reference cell d (cell under consideration) and the other closest base station. In the S1 region we will consider the user server base station as the closest one [3]. We have to mention that we assume that users in this region cannot communicate with the reference cell.

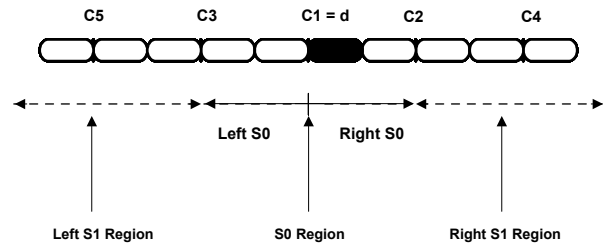


Fig. 3. The microcells model (5 out of 9 microcells are shown).

Let be S the desired signal level. Then, the interference from an active user communicating with the home cell will be also S . A user i in the S0 region will not communicate with the reference cell d but rather with base station m , if $\phi(\xi_{id} - \xi_{im}, r_{id} / r_{im}) = 1$ for

$$L(r_{id}, r_{im}) 10^{(\xi_{id} - \xi_{im}) / 10} \leq 1 \quad (9)$$

and $\phi(\xi_{id} - \xi_{im}, r_{id} / r_{im}) = 0$ otherwise.

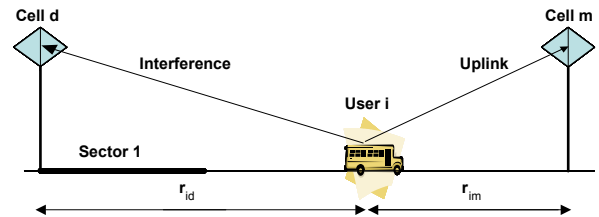


Fig. 4. Schematic diagram of base stations and mobiles for the groove road microcells.

It is assumed that the number of users in each sector is N_u and that the activity factor is α . For a uniform distribution of users, density of users in each sector is $\rho = N_u/R$ users per unit length.

Then, for the right part of S0 the expected value of I_{S0} is given as:

$$E[I_{S0}]_r = \alpha\rho \int_{S0} L(r_{id}, r_{im}) f\left(\frac{r_{id}}{r_{im}}\right) dr \quad (10)$$

where

$$f\left(\frac{r_{id}}{r_{im}}\right) = E\left[10^{(\xi_{id}-\xi_{im})/10} \phi(\xi_{id}-\xi_{im}, r_{id}/r_{im})\right] \quad (11, 12)$$

$$= e^{(\beta\sigma)^2/2} Q\left[\sqrt{\sigma^2} \ln 10/10 - \frac{10}{\sqrt{\sigma^2}} \log_{10}\{1/L(r_{id}, r_{im})\}\right]$$

being $\beta = \ln 10/10$. The general value of σ^2 is given as:

- If $(r_{id}$ and $r_{im} \leq R_b)$ then $\sigma_{id} = \sigma_1$, also $\sigma_{im} = \sigma_1$ then
$$\sigma^2 = 2(1 - C_{dm})\sigma_1^2 \quad (13)$$

where C_{dm} is the correlation coefficient between the random variables ξ_{id} and ξ_{im} .

- If $r_{id} \leq R_b$ and $r_{im} > R_b$ or $r_{id} > R_b$ and $r_{im} \leq R_b$ then the value of σ^2 is given by

$$\sigma^2 = (\sigma_1 - \sigma_2)^2 + 2(1 - C_{dm})\sigma_1\sigma_2. \quad (14)$$

- If $r_{id} > R_b$ and $r_{im} > R_b$ then $\sigma_{id} = \sigma_2$, and also $\sigma_{im} = \sigma_2$ then

$$\sigma^2 = 2(1 - C_{dm})\sigma_2^2. \quad (15)$$

$Q(x)$ is given by

$$Q(x) = \int_x^\infty e^{-v^2/2} dv / \sqrt{2\pi}. \quad (16)$$

The expected value of I_{S1} due to right part of the S1 region is approximated as

$$E[I_{S1}]_r \approx \alpha\rho \int_{S1} L(r_{id}, r_{im}) E\left[10^{(\xi_{id}-\xi_{im})/10}\right] dr. \quad (17)$$

The expected value of the intercellular interference from the right side of the regions S0 and S1 is then

$$E[I]_r = E[I_{S0}]_r + E[I_{S1}]_r. \quad (18)$$

For the left part of S0 the expected value of I_{S0} is given as

$$E[I_{S0}]_l = \alpha\rho Sll \int_{S0} L(r_{id}, r_{im}) f\left(\frac{r_{id}}{r_{im}}\right) dr \quad (19)$$

where Sll is the side lobe (back lobe) level of the directive antenna used in each sector. And the expected value of I_{S1} due to the left part of S1 is given as

$$E[I_{S1}]_l \approx \alpha\rho Sll \int_{S1} L(r_{id}, r_{im}) E\left[10^{(\xi_{id}-\xi_{im})/10}\right] dr. \quad (20)$$

The expected value of the intercellular interference from the left side of the regions S0 and S1 is

$$E[I]_l = E[I_{S0}]_l + E[I_{S1}]_l. \quad (21)$$

Thus the expected value of the total interference from the left and right sides is given as

$$E[I]_{inter,t} = E[I]_r + E[I]_l. \quad (22)$$

The expected value of the total intercellular interference power is given as

$$E[Ip]_{inter} = S E[I]_{inter,t}. \quad (23)$$

The intracellular interference power is proportional to source activity factor, number of users and the side lobe level. It is given by

$$I_{intra} \approx \alpha SN_u (1 + Sll). \quad (24)$$

Finally, the total interference-to-signal ratio is given by

$$\frac{I_t}{S} = \frac{I_{intra}}{S} + \frac{E[Ip]_{inter}}{S}. \quad (25)$$

So the uplink carrier-to-interference ratio $(C/I)_{up}$ is given as

$$(C/I)_{up} = S/I_t \quad (26)$$

and $(E_b/N_0)_{up}$ is given as

$$(E_b/N_0)_{up} = (C/I)_{up} G_p \quad (27)$$

where G_p is the processing gain.

For a voice user that has a velocity of 120 km/h, the relation $(E_b/N_0)_{up}$ has to be 7 dB or more [8] and for a data user with a bit rate of 144 kbits/sec., the ratio $(E_b/N_0)_{up}$ has to be 3 dB or more [8]. The expected number of users $E(N_u)$ can be calculated from (27). The procedure to obtain the variance of the number of users is as follows.

The variance of I_{S0} due to right part of S0 is given as

$$\text{var}[I_{S0}]_r = \rho \int_{S0} [L(r_{id}, r_{im})]^2 \left\{ \alpha g\left(\frac{r_d}{r_m}\right) - \alpha^2 f^2\left(\frac{r_d}{r_m}\right) \right\} dr \quad (28)$$

where

$$g\left(\frac{r_d}{r_m}\right) = E\left[10^{(\xi_{id}-\xi_{im})/10} \phi(\xi_{id}-\xi_{im}, r_{id}/r_{im})\right]^2 \quad (29)$$

$$= e^{2(\beta\sigma)^2} Q\left[\sqrt{\sigma^2} \ln 10/5 - \frac{10}{\sqrt{\sigma^2}} \log_{10}\{1/L(r_{id}, r_{im})\}\right] \quad (30)$$

The variance of I_{S1} due to right part of S1 is given as

$$\text{var}[I_{S1}]_r \approx \rho \int_{S1} [L(r_{id}, r_{im})]^2 \left\{ \alpha E\left[10^{(\xi_{id}-\xi_{im})}\right]^2 - \alpha^2 E^2\left[10^{(\xi_{id}-\xi_{im})}\right] \right\} dr \quad (31)$$

The variance of I_{S0} due to left part of S0 is given as

$$\text{var}[I_{S0}]_l = \rho S l l \int_{S0} [L(r_{id}, r_{im})]^2 \left\{ \alpha g\left(\frac{r_d}{r_m}\right) - \alpha^2 f^2\left(\frac{r_d}{r_m}\right) \right\} dr \quad (32)$$

The variance of I_{S1} due to left part of S1 is given as

$$\text{var}[I_{S1}]_l \approx \rho S l l \int_{S1} [L(r_{id}, r_{im})]^2 \left\{ \alpha E\left[10^{(\xi_{id}-\xi_{im})}\right]^2 - \alpha^2 E^2\left[10^{(\xi_{id}-\xi_{im})}\right] \right\} dr \quad (33)$$

Thus the total variance due to the total region S0 and S1 is given by

$$\text{var}[I]_t = \left\{ \text{var}[I_{S0}]_r + \text{var}[I_{S1}]_r \right\} + \left\{ \text{var}[I_{S0}]_l + \text{var}[I_{S1}]_l \right\}. \quad (34)$$

The variance of the number of user $\text{var}(N_u)$ is calculated as

$$\text{var}(N_u) = \text{var}[I]_t E(N_u). \quad (35)$$

Finally, the outage probability is calculated as

$$P_r = Q\left[\frac{E(N_u) - N_u}{\sqrt{\text{var}(N_u)}}\right] \quad (36)$$

and the F factor is calculated as

$$F = \frac{\text{Inter-cellular Interference}}{\text{Intra-cellular Interference}} = \frac{E[I_p]_{\text{inter}}}{I_{\text{intra}}}. \quad (37)$$

4. Numerical Results

A nine microcells model is used in the analysis. We have assumed that the W-CDMA chip rate is 3.84 Mchip per sec. For our calculations, some reasonable figures are applied. The azimuth side lobe level (back lobe) is assumed to be -15 dB, the correlation coefficients are $C_{dm} = 0.0$, we consider $s = 2$, $n = 0.04$ dB/m, $\sigma_1 = 2$ dB, $\sigma_2 = 2$ dB, $R_b = 300$ m and $R = 1000$ m unless other values are mentioned. We assume that the accepted outage probability is 1% and that the capacity of the sectors is calculated at this probability.

Tab. 1 gives the calculated values of $E[I]_t$, $\text{var}[I]_t$ and the F factor for different conditions assuming $\alpha = 0.5$.

Conditions	$E[I]_{\text{inter,t}}$	$\text{var}[I]_t$	F
$s = 2, n = 0.02$ dB/m	0.0557	0.0202	0.108
$s = 2, n = 0.04$ dB/m	0.0277	0.0100	0.054
$s = 2, n = 0.06$ dB/m	0.0183	0.0066	0.035
$s = 2, n = 0.04$ dB/m, $\sigma_1=2$ dB, $\sigma_2= 4$ dB	0.0278	0.0114	0.054

Tab. 1. The value of $E[I]_t$, $\text{var}[I]_t$ and the F factor for different conditions.

We present first the case of voice users ($G_p = 256$) assuming that the activity factor α is 0.5.

Fig. 5 shows the outage probability of the sector. We can notice that the sector capacity is 91 voice users while the average capacity (50% outage) is 94 users. Thus the practical capacity is 96% of the average one which is an advantage in this case. This is because of the very steep curve, which has been also noticed in cigar shaped micro-cells in highways [4]. In macro-cellular environment, practical capacity is of the order 60 to 70 % of the average one.

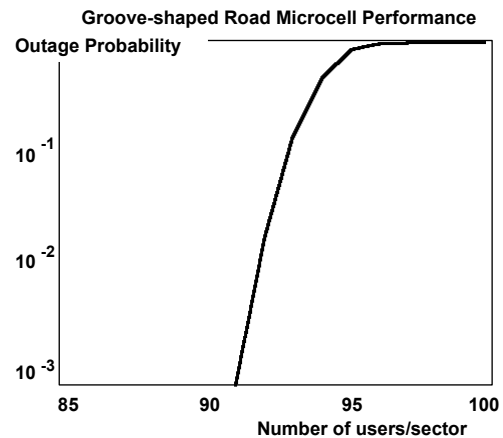


Fig. 5. The outage probability of the sector (voice users only).

Fig. 6 shows the effect of the sector range. We can notice that the capacity of the sector increases with the increment of the sector range R . Fig. 7 shows the effect of the side lobe (back lobe) level on the sector capacity. Reducing the side lobe (back lobe) level will increase the capacity of the sector. An antenna with side lobe (back lobe) level of -15 dB or better is a good choice.

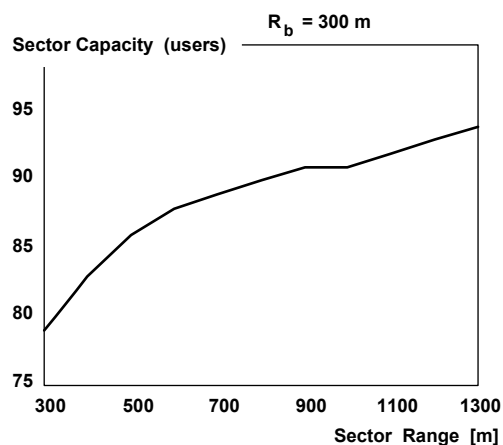


Fig. 6. Sector performance for different values of the sector range R .

To study the effect of the bend loss, we assume that there is a bend between cells C1-C2. From Fig. 8, we notice that the higher is the bend loss, the higher is the sector capacity.

Next, we consider data users case where $G_p = 26.66$ and $\alpha = 1$. Fig. 9 shows the performance of the sector. It can be noticed that, the sector capacity is 12 data users.

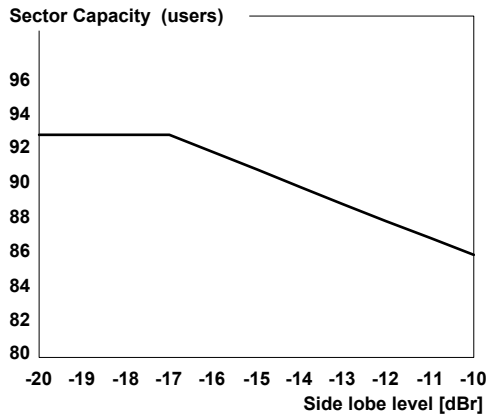


Fig. 7. Effect of the antenna side lobe level on the sector capacity.

5. Conclusion

We have presented a model that gives the capacity and interference statistics of a W-CDMA groove road cigar-shaped microcells. The effect of the sector range and the side lobe level of the directive antenna is studied. The capacity of the sector is studied using a two-slope propagation model with lognormal shadowing and bends loss.

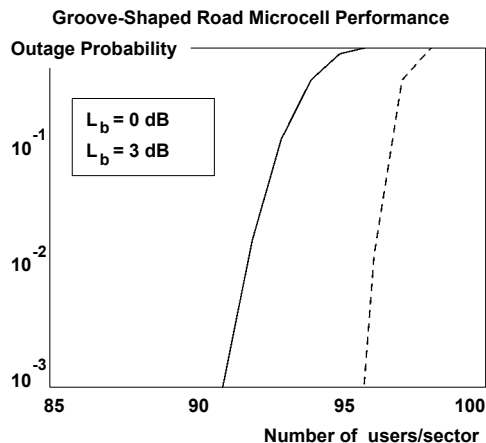


Fig. 8. Effect of the groove road bends loss.

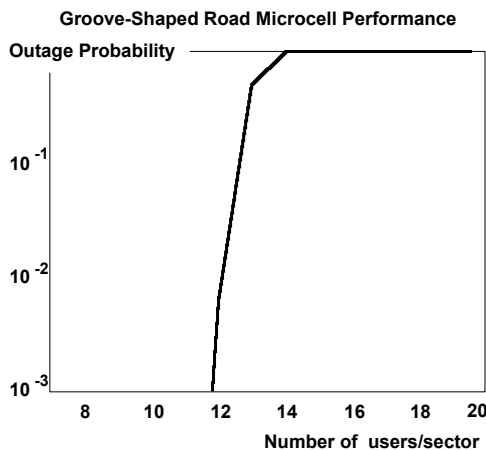


Fig. 9. The outage probability of the sector (data users only).

It has been noticed that:

- Increasing the sector range R , increases the sector capacity.
- With antenna side lobe (back lobe) level of -15 dB, the capacity is quasi the maximum possible.
- The lower is the bend loss; the lower is the sector capacity.
- Increasing s_1 and s_2 will reduce the sector capacity.
- The microcells that most strongly contribute to the interference are the three cells those exist in the center of the nine microcells model.

References

- [1] CHO, H. S., CHUNG, M. Y., KANG, S. H., SUNG, D. K. Performance analysis of cross- and cigar shaped urban microcells considering user mobility characteristics. *IEEE Transactions on Vehicular Technology*. 2000, vol. 49, no. 1, p 105 – 115.
- [2] MIN, S., BERTONI, H. L. Effect of path loss model on CDMA system design for highway microcells. In *Proceedings of the 48th Vehicular Technology Congress*. Ottawa (Canada), 1998, p 1009 – 1013.
- [3] HASHEM, B., SOUSA, E. S. Reverse link capacity and interference statistics of a fixed-step power-controlled DS/CDMA system under slow multipath fading. *IEEE Transactions on Communication*. 1999, vol. 47, no. 12, p. 1905 – 1912.
- [4] AHMED, B. T., RAMÓN, M. C., ARIET, L. H. Shaped W-CDMA cells performance in highways. *IJECE*. 2002, vol. 1, no. 2, p. 80 to 84.
- [5] AHMED, B. T., RAMÓN, M. C., ARIET, L. H. W-CDMA uplink capacity and interference statistics of a long tunnel cigar-shaped microcells. *JCN*, submitted.
- [6] OHTAKI, Y., SENGOKU, M., SAKURI, K., YAMAGUCHI, Y., ABE, T. Propagation characteristics in open-groove waveguides surrounded by rough sidewalls. *IEEE Transactions on Electromagnetic Compatibility*. 1990, vol. 32, no. 3, p 177 – 184.
- [7] ZHANG, Y. P., HWANG, Y., PARSONS, J. D. UHF radio propagation characteristics in straight open-groove structure. *IEEE Transactions on Vehicular Technology*. 1999, vol. 48, no. 1, p. 249 – 254.
- [8] MELIS, B., ROMANO, G. UMTS W-CDMA: Evaluation of radio performance by means of link level simulations. *IEEE Transactions on Personal Communications*. 2000, vol. 7, no. 3, p. 42 – 49.

About Authors...

For authors’ biographies, see *Radioengineering*, 2003, vol. 12, no. 3, p. 19.